

# DEAP DIVE: Dataset Investigation with Vision transformers for EEG evaluation

Annemarie Hoffsommer<sup>1\*</sup>, Helen Schneider<sup>1\*</sup>, Svetlana Pavlitska<sup>1,2</sup>, J. Marius Zöllner<sup>1,2</sup>

<sup>1</sup> Karlsruhe Institute of Technology (KIT), Germany

<sup>2</sup> FZI Research Center for Information Technology, Germany

helen.schneider@kit.edu

## Abstract

Accurately predicting emotions from brain signals has the potential to achieve goals such as improving mental health, human-computer interaction, and affective computing. Emotion prediction through neural signals offers a promising alternative to traditional methods, such as self-assessment and facial expression analysis, which can be subjective or ambiguous. Measurements of the brain activity via electroencephalogram (EEG) provides a more direct and unbiased data source. However, conducting a full EEG is a complex, resource-intensive process, leading to the rise of low-cost EEG devices with simplified measurement capabilities. This work examines how subsets of EEG channels from the DEAP dataset can be used for sufficiently accurate emotion prediction with low-cost EEG devices, rather than fully equipped EEG-measurements. Using Continuous Wavelet Transformation to convert EEG data into scaleograms, we trained a vision transformer (ViT) model for emotion classification. The model achieved over 91,57% accuracy in predicting 4 quadrants (high/low per arousal and valence) with only 12 measuring points (also referred to as channels). Our work shows clearly, that a significant reduction of input channels yields high results compared to state-of-the-art results of 96,9% with 32 channels. Training scripts to reproduce our code can be found here: <https://gitlab.kit.edu/kat/aifb/ATKS/public/AutoSMiLeS/DEAP-DIVE>.

## 1. Introduction

The ability to predict human emotions accurately from neural signals holds potential for various fields, including (mental) health[25], human-computer interaction[45], and affective computing[24]. Traditionally, emotion recognition has relied on subjective or ambiguous methods, such as self-assessment and facial expression analysis[37]. While

\*These authors contributed equally to this work

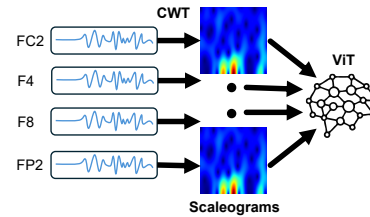


Figure 1. Concept diagram for exemplary approach with 4 channels. Each input consists of only 4 channels with a recording length of one video watched by one person. Each channel is transformed into a separate scaleogram through a CWT. All 4 scaleograms are used as input for the ViT.

these methods provide valuable insights, they are limited by their dependence on interpretation, leading to inconsistencies and potential biases[7]. Importantly, methods such as Electroencephalography (EEG) provide a direct and objective approach to analyzing neural activity and assessing emotional states by measuring the brain’s electrical signals. This method mitigates the limitations of traditional techniques, such as subjective biases and inconsistencies.

However, despite the advantages of EEG-based emotion prediction, a full-scale EEG setup is often resource-intensive. Medical-grade EEG devices, typically used in clinical settings, require specialized training, costly equipment, and extensive preparation due to the high number of channels involved (up to 60 electrodes). This complexity renders it impractical for application in remote settings, home healthcare environments, regions with limited access to medical resources, or by researchers from different disciplines lacking specialized medical expertise. To address this, there is an increasing interest in rendering portable, low-cost EEG devices usable in practical applications, particularly for emotion recognition [21], [9]. These devices, though limited in terms of the number of electrodes, offer a more accessible solution. An open research challenge involves the use of EEG-devices in delivering reliable predictions of emotions with fewer input channels[20].

This work explores how subsets of EEG channels from the DEAP dataset [23], a widely used benchmark for emotion recognition [4, 36, 40], can be used to achieve accurate emotion prediction, even with low-cost, simplified EEG devices. We investigate the balance between minimizing the number of input channels and maintaining prediction accuracy, with a focus on making EEG-based emotion recognition more accessible and practical in real-world scenarios.

A key element of our approach involves mapping EEG signals to emotions. Emotions are complex, dynamic processes that often defy simple categorization[6]. However, by employing advanced signal processing techniques, such as Continuous Wavelet Transformation (CWT)[30], which captures temporal dependencies in EEG signals, we can transform these signals into images, known as scaleograms. Therefore, through the transformation of EEG data into CWTs we obtain a visual representation of the DEAP Dataset. Scaleograms are considered meaningful input for data with wavelet characteristics (e.g. EEGs) as they provide direct knowledge to relevant features of the data - the frequencies over time. These images are then used to train a vision transformer [10], a model architecture designed to capture both temporal and spatial dependencies in data. Our approach is displayed visually in an exemplary concept diagram in Figure 1. By pairing CWT with the ViT, we aim to capture the underlying patterns in brain activity that correspond to emotional states. CWT has been used in recent studies combined with convolutional neural networks (CNNs)[14], support vector machines (SVMs) [12], or standard statistical methods[29].

Our contributions are threefold. **First**, our work is the first to use CWT combined with vision transformers for emotion recognition and reaching SoTA results. **Second**, we offer insights into the minimal requirements for accurate brain-computer interfacing by analyzing different subsets of EEG-channels. We show that using only 12 channels achieves results of 91.57% accuracy close to SoTA-results of 96.90% with 32 channels. **Third**, we are the first, to the best of our knowledge, to provide a baseline for regression on valence and arousal for DEAP with an RMSE of 0.57.

## 2. Related Work

### 2.1. Emotion Recognition

Accurately labeling and classifying emotions, along with understanding their relationships and proximity, is a complex and often ambiguous task, as no clear metric exists. The Circumplex Model of Affect, proposed by Russell in the 1970s [34] and still widely used today, serves as a tool for defining and organizing emotions. This model classifies emotions on a continuous, two-dimensional scale. The horizontal axis - **valence** - represents the range from negative to positive emotions, while the vertical axis - **arousal** - mea-

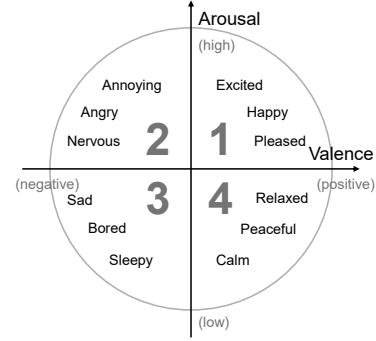


Figure 2. Russell’s Circumplex Model of Affect [8] showing four quadrants(Q) used for our classification.

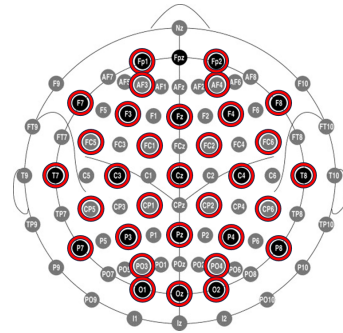


Figure 3. International 10-20-System for EEG-channel placement modified from [31] to highlight channels recorded in DEAP.

asures the level of activation, from calmness or sleepiness to excitement or arousal (see Figure 2).

Classifying emotions has been done among others with facial configurations [43],[47], physiological signals (e.g. heartbeat [38], galvanic skin response[32], EEG[13]), and body posture [35]. In our work, we analyze how EEG-data can give insights into what is happening in the brain during emotional occurrences and how new techniques such as vision transformers can help in making low-cost EEG-recordings more useful in affective research.

### 2.2. Datasets for Emotion Recognition using EEG

Commonly used datasets for sentiment analysis with EEG data include SEED&SEED-IV[46], [11], MAHNOB-HCI[39] and DEAP [23]. The SEED dataset utilizes movie clips to evoke emotions labeled as positive, negative, and neutral (or happy, sad, fearful, neutral in SEED-IV). However, with only 15 participants, SEED has fewer subjects compared to DEAP, which is seen as a limitation for cross-subject validation. The MAHNOB-HCI dataset, which also uses movie clips to elicit emotions, includes 27 subjects and labels emotions based on liking and disliking. This labeling approach was not chosen for our work due to its misalignment with the intended Circumplex Model of Affect.

Table 1. Related Work on Emotion Classification on the DEAP Dataset

Author & Citation	Year	Accuracy ↑ 4-Class (%)	Accuracy ↑ Binary Valence (%)	Accuracy ↑ Binary Arousal (%)	Accuracy ↑ Combined Binary (%)	Method	Number Channels
Li et al. [26]	2016	-	72.06	74.12	53.41	CRNN	32
Wang et al. [44]	2020	56.93	66.51	65.75	43.73	Transformer	32
Marjit et al. [29]	2021	83.52	88.28	90.63	80.00	MLP	32
Arjun et al. [3]	2022	-	65.90	69.50	45.80	LSTM	32
Quan et al. [33]	2023	69.02	81.19	79.59	64.62	VAE	32
Tao et al. [40]	2023	-	97.93	97.98	95.96	Attention, CNN	32
Fan et al. [13]	2024	-	98.61	98.63	97.26	ResNet	40
<b>Ours</b>		<b>91.57</b>				<b>ViT</b>	<b>12</b>

Table 2. Related Work on Emotion Classification with Wavelet Transformations (WT) on the DEAP Dataset

Author & Citation	Year	Accuracy ↑ 4-Class (%)	Accuracy ↑ Binary Combined (%)	Method	Cross Subject	Number Channels
Gupta et al. [16]	2019	72.07	-	FlexibleWT and Random Forest	yes	40
Islam et al. [18]	2019	62.30	-	DiscreteWT and KNN	no	10
Liu et al. [27]	2020	-	96.31	Multi-level features guided Capsule Network	no	32
Garg et al. [14]	2020	-	56.44	Scaleograms and CNN	no	40
A.-Conejo et al. [1]	2023	83.43	-	Scaleograms and GoogLeNet	no	32
Bagherzadeh et al. [5]	2023	96.90	-	Scaleograms and CNN Majority Voting	no	32
<b>Ours</b>		<b>91.57</b>		<b>Scaleograms and ViT</b>		<b>12</b>

The DEAP dataset comprises data from 32 participants, with 40 different measurements (also referred to as channels). These include 32 EEG channels (see Figure 3), along with additional physiological signals, e.g. electrooculography (eye movement), electromyography (muscle activity), galvanic skin response, blood volume pressure, respiration, and temperature. In DEAP, each participant watched 40 one-minute music videos, selected to evoke a range of emotional responses. After viewing each video, participants rated their emotional state in terms of valence, arousal, dominance, and liking, using a self-assessment method.

For this work, we used the preprocessed DEAP dataset, already prepared via data reordering, downsampling, artifact removal, band-pass filtering, and averaging to a common reference (see [23] for more details).

The number of selected videos in the DEAP Dataset is slightly unbalanced per quadrant (class), while the quadrants are Q1: High Arousal & High Valence - Q2: High Arousal & Low Valence - Q3: Low Arousal & Low Valence - Q4: Low Arousal & High Valence (see Figure 2). The following numbers of videos were available in the Dataset with each participant watching all of them: 8 in Q1, 12 in Q2, 10 in Q3 and 10 in Q4. Due to the insignificant low imbalance, we did not employ dataset balancing techniques.

### 2.3. State of the art for DEAP dataset classifications

Previous work for classification on the DEAP dataset can be seen in Table 1. The four class accuracy refers to classification of affect into the four quadrants of Q1, Q2, Q3 and Q4 as mentioned above. Therefore predicting valence

and arousal simultaneously. Best results are achieved by our vision transformer with 91.57% accuracy compared to 83.52% accuracy reached using a Multi-Layer Perceptron (MLP)[29]. The binary classifications of valence is predicting either high or low and for the binary classifications of arousal respectively. For comparability to the four class approach, the combined binary accuracy is calculated as the probability of the model for binary valence and the model of binary arousal to classify the same data as a combined model correctly into the four quadrants. The accuracy is calculated by multiplying the accuracy of binary valence and binary arousal. The intention of the binary combined accuracy was solely to provide a theoretical reference for comparison within the 4-class classification task, therefore it was not computed for the proposed model.

### 2.4. State of the art DEAP classification using CWT

Previous work of classifying the DEAP dataset including wavelet transformations for preprocessing are shown in Table 2. Using CWT combined with a vision transformer results in 91.57% accuracy (only 12 channels) reaching near to state-of-the-art results of 96.9% accuracy (32 channels) with a majority voting of CNNs[5], despite significantly lower amount of input and utilizing only one architecture. The highest 4-class accuracy reported by [5] was achieved using a wavelet transformation. Building on this, the EEG data in this work was represented as scaleograms obtained through a wavelet transformation.

## 2.5. State of the art for DEAP dataset regression

To our knowledge there is no work available that also predicts continuous values from the DEAP dataset. [47] predicts the continuous valence of the MAHNOB-HCI dataset by using facial expression and EEG Data. Using a subset of the DEAP Dataset only containing the EEG channels we achieved a Root Mean Squared Error (RMSE) of 0.57.

## 3. Methods

A CWT was applied to each normalized measurement in order to generate a scaleogram. The continuous wavelet transformation [30], [15], decomposes a given signal into the frequency components and their magnitude of the signal at each time. This 3D Data can be plotted as a 2D scaleogram with time and frequency as axis and the magnitude as color. Please note that in order to gain a result containing information of time and frequency the CWT loses resolution in difference to a fully reversible Fourier Transformation.

Each resulting image corresponds to one electrode recording from a single participant while watching a one-minute video. The processed images were subsequently input into a vision transformer model. It was possible to choose different subsets of channels and build models using only specific single or groups of measurements. An exemplary approaches 4 channels can be seen in Figure 1.

Although the CWT introduces a slight loss of information into the system, this trade-off was considered acceptable. As the gain in time-domain information, combined with the transformer’s ability to process temporal dependencies, was deemed to be beneficial.

We formulate the emotion recognition problem as a 4-class classification task, with the following labels: high arousal-low valence, high arousal-high valence, low arousal-low valence, low arousal-high valence. The VAQ\_Estimate of the video (Valence Arousal Quadrant) was selected by the DEAP experimenters and was preferred as label over the self assessment manikin (SAM) labels (labeled by the participants) as it is less dependent on differing and inconsistent ratings of persons. If not otherwise stated in Chapter 5.3, the VAQ\_Estimate was chosen as label.

A vision transformer (Linformer) model was employed. Vision transformers [10] apply the self-attention mechanism of transformers[42]. ViTs partition images into fixed-size patches, linearly embedding them into sequences related to tokens used in language models [10]. This approach allows the model to capture long-term dependencies as well as global and spectral context effectively [42].

A linear classification layer was added to adapt the network for a 4-class classification task. The target classes were based on high/low arousal and high/low valence. Unless stated otherwise in 5.3, the VAQ\_Estimate was used as the label for classification.

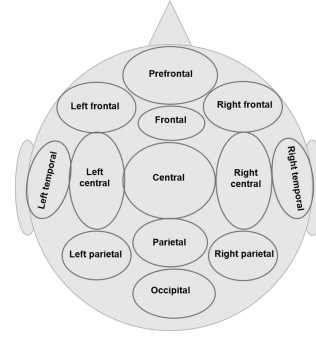


Figure 4. EEG Placement and the corresponding brain region [28].

## 4. Experiment Setup

For our experiments, the entire data of the DEAP-dataset was split into  $k=5$  cross validation folds. The train-test split was conducted not dependent on participant ID. This means that part of the data stemming from a single participant could be in test-split, while the rest of the data from this participant could be in the train-split. This configuration allows for an evaluation of how well the models could generalize when baseline data from a person is available for training. The images obtained by the CWT were bi-linear resized to 224x224 pixels.

For the classification experiments different setups were chosen to evaluate the use of only one channel, subsets of the entire channels and differences between using SAM-labels and VAQ labels. Finally, a regression was conducted in order to have a more fine-grained evaluation of emotional experiences.

For all classification experiments, a learning rate scheduler and the Adam optimizer [22] as well as Cross Entropy Loss was employed for the training. Each experiment used 5-fold cross-validation ( $k=5$ ). Early stopping was implemented, with training halted if the test loss did not improve after five consecutive epochs of exceeding the minimum observed test loss.

### 4.1. Classification - Single Channel Experiments

For the single channel experiments, each EEG channel was tested individually to assess its ability to predict emotions using the smallest available data subset.

### 4.2. Classification - Channel Subsets Experiments

In order to evaluate how different numbers of EEG-channels result in different accuracies, the following subsets were employed for training:

**All Data:** All available data from the DEAP dataset was used for this experiment including EEG and other physiological signals.

**Muse-12/8/4 Electrodes and Emotiv Testing:** To evaluate the performance of low-budget EEG devices with

fewer electrodes, two commonly used devices were selected: the Muse S\* (with 4 electrodes - AF7, AF8, TP9, TP10) and the Emotiv\* (with 12 electrodes, (AF3, F7, F3, FC5, T7, P7, O1, O2, P8, T8, FC6, F4, F8, AF4)). Since the exact electrode placements of the Muse S are not available in the DEAP dataset, the closest corresponding electrodes were used. The experiments tested the three nearest (setup "Muse-12" - AF3, AF4, FP1, FP2, F7, F8, P7, P8, CP5, CP6, T7, T8), two nearest (setup "Muse-8" - AF3, AF4, F7, F8, P7, P8, T7, T8), and the single nearest (setup "Muse-4") electrodes to match the Muse S setup. As the nearest electrodes to the Muse were unclear to determine there are two Version 4a (AF3, AF4, P7, P8) and 4b (F7, F8, T7, T8).

**PCA-12/4 Testing:** A Principal Component Analysis (PCA) was applied to the entire dataset as a standard method to identify the most relevant features. The 12 (setup "PCA-12") or 4 (setup "PCA-4") most relevant channels, determined based on the explained variance ratio, were grouped together and tested.

**EEG-Only Setup:** This experiment used only channels 1-32, which correspond to the EEG electrodes, excluding other physiological measurements.

**Non-EEG-Only Setup:** In this configuration, only channels 33-40 were used, corresponding to non-EEG physiological measurements.

**Grouped Channels:** EEG channels were grouped by the brain regions the placements correspond to, and each group's performance was tested individually. See Figure 4 for the different regions.

### 4.3. Classification - Differences between SAM and VAQ labels

In this setup, the SAM-labels were used instead of the VAQ-labels. SAM labels were given individually by each participant, while the VAQ labels were given by the experimenters. The objective was to investigate potential significant differences between the two labeling methods and gain deeper insights into the limitations of self-assessed data.

For the SAM labels, each video was classified by each participant individually based on the assigned valence and arousal scores of their self-assessment. SAM data ranges from 1 to 9 and was collected by participants selecting a position on a continuous horizontal scale between five manikins, with a distance of 1.6 units between each manikin. To compare the SAM and VAQ label data, the threshold for classifying a video as high or low valence/arousal was set at 5, as in the original DEAP study.

### 4.4. Regression Experiments

For the regression task only SAM labels were used, as they provide the only continuous values in the dataset. For train-

Table 3. Accuracy ( $\uparrow$ ) for single experiments

Channels	Fold 1	Fold 2	Fold 3	Fold 4	Fold 5	Mean
channel 33	70.38	64.36	70.00	<b>72.44</b>	71.67	69.37
channel 34	37.05	38.33	31.41	34.62	37.31	35.74
channel 37	28.21	30.26	36.15	33.97	34.36	32.19
channel 33 cross person	71.79	68.57	61.25	69.17	<b>78.33</b>	69.82

ing, the loss function was adjusted to the Huber Loss to account for outliers that are expected due to human factors and the Root-Mean-Squared-Error (RMSE) was used as metric. As it was observed that regressions tend to train longer, the early stopping threshold was adjusted to 10 consecutive epochs compared to the 5 in the classification settings.

## 5. Results

Defining what qualifies as relevant, significant, or sufficient for this study does not have a precise answer. Previous works (see Tables 1 and 2) do not contain a strict definition of a relevant result. To overcome this problem, we introduce the following new definition: in this work, the results for predicting four classes were considered relevant when the accuracy exceeded twice the expected random accuracy, effectively surpassing the 50% threshold. We are aware that due to the unbalanced dataset, this is not an exact calculation of chances. Serving the purpose of setting a lower bound, though, this calculation was considered sufficient.

For regression within the 9x9 area, the expected RMSE for the given data is 3.399. Accordingly, results were deemed relevant when the RMSE was lower than 1.6995, which is half of the expected RMSE value.

### 5.1. Classification - Single Channel Experiments

Only one channel, Channel 33 produced a sufficiently high classification accuracy when used as the sole input. This channel, representing horizontal eye movement (hEOG), is not typically part of an EEG setup. With an accuracy exceeding 70% for classifying four classes, it provides a partial answer to the question of how little input is needed to achieve meaningful predictions. Other channels did not yield an accuracy considered as significant.

As follow up we conducted a cross-person experiment for the single channel of horizontal eye movement. In this setup the test and train split was depending on the persons. Meaning that no data from a person selected in test was used for training of the model. The accuracy remained the same for the cross-person setting of channel 33, one fold even surpassed the previous experiments. This suggests that the eye movement could be a beneficial measurement for low-budget EEG-devices as it provides a solid basis for classification. However, it is yet to be determined whether the eye-movement-model predicted an emotion or rather just

\*<https://choosemuse.com/>

\*<https://www.emotiv.com/>

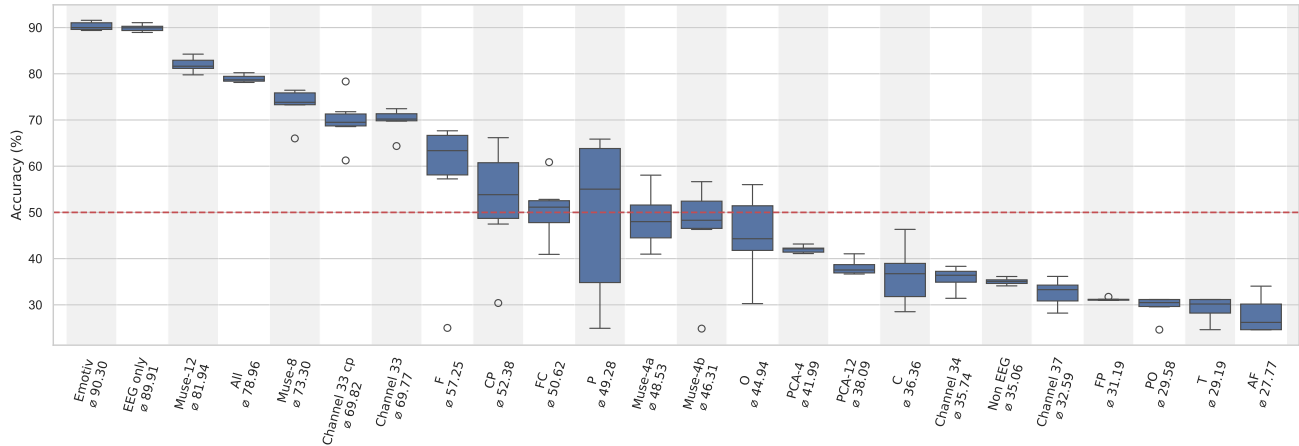


Figure 5. Classification experiments with VAQ labels - labels given by the experimenters. Results of Table 3, 6 and 5 are presented visually by their 5 folds locality, spread and skewness through their quartiles. Experiments are ordered by descending mean of their 5 folds accuracy( $\uparrow$ ) respectively. The mean ( $\emptyset$ ) is shown after the experiment name in the labels of the horizontal axis. The dashed red line indicates the threshold of the double of random results. The data shows the first 6 experiments clearly over the threshold line in all 5 folds respectively. Outliers that differ significantly from the other folds are depicted as circles. Interestingly, the grouped "O"-channels perform only slightly below the threshold with a mean of 44.94% even though the group only contains 3 channels. The Emotiv-channels perform best with a mean of 90,3% in accuracy with only 12 channels as input.

learned which eye movements correspond to which videos and what label the video corresponded to. For detailed accuracy of each fold of the best single channel results, see Table 3. A box-plot overview of all conducted experiments (including the best four single channel results) and their means over all 5 folds can be seen in Figure 5. Channel 33 clearly lies in the top 7 results of all experiments.

For completeness, we experimented with cross-person setting by leaving 6 people out for each fold for validation. For channel 33 this resulted in a mean accuracy of 71.9%.

## 5.2. Classification - Channel Subsets Experiments

**All Data** - When all available channels were utilized, the classification accuracy reached approximately 80%.

**Muse-12/8/4 Electrodes** - Using 12 electrodes resulted in one of the best-performing configurations with a maximum accuracy of 84%. Reducing the input to 8 electrodes caused an 8% drop in accuracy, reaching 76%. However, further reducing the input to 4 electrodes led to a more substantial drop in accuracy, falling by approximately 20% to 58-56%. This indicates that the model's performance is more resilient when reducing from 12 to 8 electrodes than when reducing from 8 to 4 electrodes. See Table 4 for comparison of accuracy across all folds and the corresponding number of channels for each channel-name. **Emotiv** - The channels corresponding to those used in the Emotiv device achieved the best classification accuracy at 91.50%. This suggests that this specific channel subset performs exceptionally well, even with significantly fewer (12 of 40) channels than the full dataset and shows one of the best trade

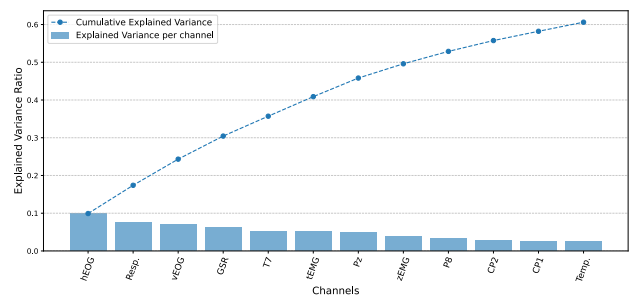


Figure 6. Explained variance for the best 12 channels obtained through PCA, with channels sorted in descending order of explained variance. The line shows the cumulative explained variance across the sorted channels. The most relevant features according to the explained variance is the hEOG (channel 33). It can be seen that the 12 channels only cumulate in a explained variance of 60%; more than half of the channels are needed to obtain a cumulative explained variance above the 80% mark.

offs between accuracy and used channels.

**PCA** - The explained variance for each channel obtained through PCA is shown in Figure 6. The ordering of explained variance across channels does not align with the ranking obtained from single-channel testing. However, the highest-ranked channel (hEOG - channel 33) is consistent between both methods. Grouping the top 12 channels resulted in a maximum accuracy of 41.04%, while grouping the top 4 led to a slightly better performance with 43.16%. Consequently, no configuration based on PCA findings is considered relevant. These results are explainable since

Table 4. Accuracy ( $\uparrow$ ) for experiments, VAQ labels

Channels	#	Fold 1	Fold 2	Fold 3	Fold 4	Fold 5	Mean
all	40	78.12	78.44	78.39	<b>80.23</b>	79.61	78.96
eeg-only	32	88.94	89.18	<b>91.06</b>	90.37	89.99	89.91
non-eeg	8	35.51	36.13	35.09	34.10	34.48	35.06
Emotiv	12	89.70	89.56	<b>91.57</b>	91.28	89.37	90.30
Muse-12	12	83.25	81.33	<b>84.25</b>	79.77	81.10	81.94
Muse-8	8	73.35	74.30	<b>76.44</b>	66.01	76.38	73.30
Muse-4a	4	40.97	52.62	43.50	58.06	47.48	48.53
Muse-4b	4	47.23	53.45	56.65	24.85	49.37	46.31
PCA-12	12	38.90	36.88	41.04	36.98	36.67	38.01
PCA-4	4	41.09	42.23	43.16	42.28	41.21	41.99

PCA is a linear feature reduction method [2], while the relationships between the features are not necessarily linear.

**EEG-only and Non-EEG only** - The EEG-only configuration achieved 91.06% accuracy, ranking second-best with no significant difference to the top result. However, this setting required more than double the number of channels compared to the Emotiv configuration for a similar outcome. In contrast, the non-EEG channel setup did not produce sufficient accuracy, despite containing channel 33.

**Grouped Channels** - Grouping the channels by location of the electrode led to ambivalent results, shown in Table 5. The groups frontal (f), parietal (p), and between central and parietal (cp) showed at least one fold with sufficient accuracy. But there is at least one fold per group where no generalization is developed. This might show that EEG features are less obvious, which might lead to an outlier-prone prediction when less training data is available. Furthermore, there are differences in the number of channels that are part of each group. All groups with relevant results are on the upper end of channel numbers, whereas the channels containing fewer channels tend to be less performing. For example, the comparison of group fc and cp shows that a group with more channels does not directly yield higher accuracy but seems more dependent on the input. Training data limitations could be a reason for more stable training with more channels; however, as the single-channel experiment showed, the used architecture is capable of performing a stable classification with only one channel.

See Figure 5 for a better insight into the experiments and a visual direct comparison between the experiments.

### 5.3. Classification - Differences between SAM and VAQ labels

Using the SAM labels resulted in mostly comparable accuracy to the VAQ label results. Taking into account that the SAM labels are more dependent on each participant and therefore have a more volatile influence on the results, the results for all channels, EEG-only, Muse-12 and Muse-8 are viewed as similar to the results of the VAQ labels. In the Emotiv and Muse-4b setup there is a similar tendency of

Table 5. Accuracy ( $\uparrow$ ) for experiments, grouped by electrode placement, VAQ labels

Channels	#	Fold 1	Fold 2	Fold 3	Fold 4	Fold 5	Mean
t	2	24.62	27.89	31.15	31.15	31.15	29.19
f	5	25.00	66.88	<b>67.66</b>	66.02	60.70	57.25
c	3	28.51	46.33	37.11	30.26	39.58	36.36
fp	2	30.96	30.96	31.73	31.15	31.15	31.19
af	2	30.96	34.04	24.62	24.62	24.62	27.77
po	2	31.15	29.81	31.15	31.15	24.62	29.19
fc	5	40.92	52.82	51.65	60.87	46.85	50.62
cp	4	55.29	30.39	47.48	<b>66.17</b>	62.57	52.38
o	3	56.01	53.60	41.14	30.26	43.67	44.94
p	5	<b>65.86</b>	64.84	60.78	24.92	30.00	49.28

Table 6. Accuracy( $\uparrow$ ) with SAM labels, Differences between the maximal Accuracies from SAM labels to VAQ labels

Channels	#	Fold 1	Fold 2	Fold 3	Fold 4	Fold 5	Diff.
all	40	76.33	77.04	78.44	78.69	78.19	-1.84
eeg-only	32	88.06	91.18	89.68	89.40	91.63	+0.57
Emotiv	12	80.71	79.87	80.45	81.40	79.48	-10.17
Muse-12	12	83.05	82.82	81.10	81.82	83.51	-0.74
Muse-8	8	70.91	35.85	73.28	76.18	72.29	-0.26
Muse-4b	4	36.12	36.12	36.12	60.34	36.21	+3.69
Channel 33	1	40.13	43.21	45.90	45.51	42.56	-26.54

fold-performance in the SAM results and the VAQ results, respectively. However the overall difference of the Emotiv-SAM and Emotiv-VAQ is much larger than the overall difference of the Muse-4b-SAM and Muse-4b-VAQ. For the Muse-4b setup an explanation could be, that the training already seems to be unstable in the original setup (see fold 4 of Muse-4b in Table 4) and the differences and uncertainties of the labeling persons are disadvantageous. This is even more reasonable as 671 out of the 1280 total scaleograms were grouped into a different quadrant by the SAM labels than by the given VAQ.

Channel 33 showed no generalization in this setup. It is possible, that the horizontal eye movement (channel 33) is corresponding to the dynamics of the presented videos more than to the experienced feelings. The drastic differing of results could support this hypothesis, if the SAM labels are assumed to be more accurate to the experienced emotions. However eye movement is used to predict emotional states in [17],[41] with high accuracy. The open question whether the experienced emotions or the video dynamics are crucial for the prediction is also relevant for the EEG channels. An interesting result regarding this question is the performance of the Occipital Lobe group 'o' in Table 5 with 56% accuracy for 3 channels. As the Occipital Lobe is associated as center of processing visual input [19].

Detailed results are shown in Table 6, a box-plot overview is provided in Figure 7.

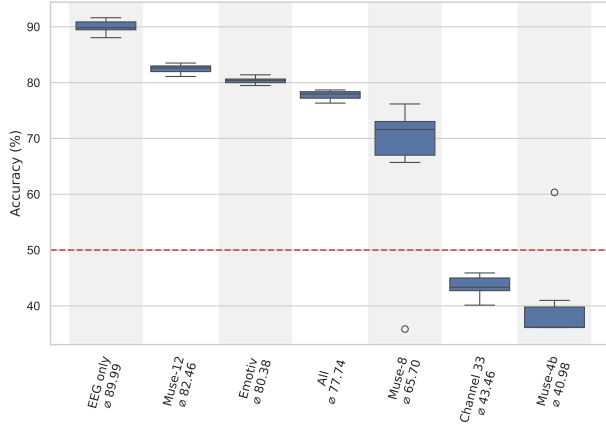


Figure 7. Box-plot and mean of the classification experiments with self-assessment labels (SAM) - labels given by participants. Results of Table 6 are presented visually as box-plots of their 5 folds and ordered by descending mean accuracy( $\uparrow$ ). The mean ( $\emptyset$ ) is shown after the experiment name in the labels of the horizontal axis. The dashed red line indicates the threshold of the double of random results. In contrast to the VAQ-label experiments seen in Figure 5 only four experiments clearly exceed the threshold line with all 5 folds.

Table 7. RMSE Values ( $\downarrow$ ) for Each Fold, Regression

Channels	#	Fold 1	Fold 2	Fold 3	Fold 4	Fold 5	Mean
all	40	1.074	1.140	1.119	1.190	1.107	1.126
eeg-only	32	<b>0.575</b>	0.611	0.624	0.612	0.604	0.605
Muse-12	12	1.156	0.926	1.020	<b>0.913</b>	1.005	1.004
Muse-8	8	1.124	1.147	1.296	1.434	1.223	1.245
Muse-4b	4	2.081	1.615	2.116	2.046	1.624	1.896
Emotiv	12	0.994	1.079	0.989	<b>0.889</b>	0.924	0.975
Channel 33	1	1.926	2.011	2.093	1.958	2.082	2.014

## 5.4. Regression Experiments

In the regression experiments, the EEG-only setup produced the best performance, achieving the lowest RMSE of 0.57. Unlike the classification task, the Emotiv setup did not perform as well, reaching an RMSE of 0.88, which is still the second-best result.

The experiments with Muse-12 and Muse-8 showed similar tendencies comparing to the classification results, with a small performance gap between them. As observed in the classification task, the performance drop when reducing to 4 channels was more substantial, indicating a larger disparity in accuracy when fewer channels were used.

For channel 33 the results were not considered relevant but are still noticeably better than random. Here it should be taken into account that one channel only provides a limited amount of data for training.

A detailed list of results is shown in Table 7, a box-plot overview is provided in Figure 8.

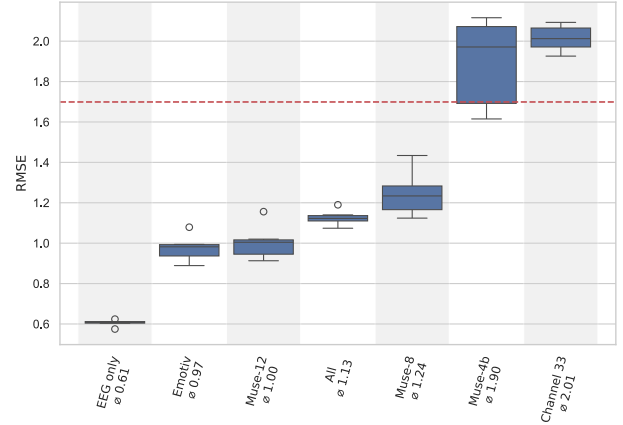


Figure 8. Box-plot and mean RMSE of the best seven regression experiments with continuous SAM labels. Results of Table 7 are presented visually as box-plots of their 5 folds and ordered by ascending mean RMSE( $\downarrow$ ). The EEG-only and Emotiv experiments show best results, with Muse-12 close to the results of Emotiv.

## 6. Conclusion

We conducted a classification and regression with different subsets of the DEAP dataset, up to testing only single input EEG channels. In conclusion, our research underscores the effectiveness of pairing scaleograms and vision transformer as well as predicting emotional states with only subsets of a common EEG.

We evaluated the trade-off between minimal input and prediction performance, evaluating models trained on varying numbers of channels. Through these analyses, we showed different configurations that can be used for portable EEG devices, enabling more accessible, reliable emotion prediction technologies, while also offering significant contributions to the broader research community.

The performance of our model showed some ambiguities with different experiment setups. Pairing subsets that achieved a high accuracy with additional channels does not always lead to better performances. Most visible was this phenomenon in experiments where all available inputs were used but did not lead to best model performance. The underlying mechanisms of this non-superpositional behavior and the factors contributing to the amplification of accuracy across certain channels remain open questions for further investigation in the field of explainable AI. An interdisciplinary approach, particularly one integrating insights from neuroscience, will be highly beneficial in advancing our understanding of these phenomena.

## Acknowledgment

This work was supported by funding from the Topic Knowledge for Action of the Helmholtz Association (HGF).

## References

- [1] Oscar Almanza-Conejo, Dora Luz Almanza-Ojeda, Jose Luis Contreras-Hernandez, and Mario Alberto Ibarra-Manzano. Emotion recognition in EEG signals using the continuous wavelet transform and CNNs. *Neural Computing and Applications*, 2023. 3
- [2] Farzana Anowar, Samira Sadaoui, and Bassant Selim. Conceptual and empirical comparison of dimensionality reduction algorithms. *Computer Science Review*, 2021. 7
- [3] Arjun, Aniket Singh Rajpoot, and Mahesh Raveendranatha Panicker. Subject independent emotion recognition using EEG signals employing attention driven neural networks. *Biomedical Signal Processing and Control*, 2022. 3
- [4] Sara Bagherzadeh, Keivan Maghooli, Ahmad Shalbaf, and Arash Maghsoudi. Emotion recognition using effective connectivity and pre-trained convolutional neural networks in EEG signals. *Cognitive Neurodynamics*, 2022. 2
- [5] Sara Bagherzadeh, Keivan Maghooli, Ahmad Shalbaf, and Arash Maghsoudi. Emotion recognition using continuous wavelet transform and ensemble of convolutional neural networks through transfer learning from electroencephalogram signal. *Frontiers in Biomedical Technologies*, 2023. 3
- [6] Raul Berrios. What Is Complex/Emotional About Emotional Complexity? *Frontiers in Psychology*, 10, 2019. 2
- [7] Yunliang Chen and Jungseock Joo. Understanding and Mitigating Annotation Bias in Facial Expression Recognition. *International Conference on Computer Vision (ICCV)*, 2021. 1
- [8] Harsh Dabas, Chaitanya Sethi, Chirag Dua, Mohit Dalawat, and Divyashikha Sethia. Emotion Classification Using EEG Signals. In *Proceedings of the 2018 2nd International Conference on Computer Science and Artificial Intelligence*, Shenzhen China, 2018. ACM. 2
- [9] Didar Dadebayev, Wei Wei Goh, and Ee Xion Tan. EEG-based emotion recognition: Review of commercial EEG devices and machine learning techniques. *Journal of King Saud University - Computer and Information Sciences*, 2022. 1
- [10] Alexey Dosovitskiy, Lucas Beyer, Alexander Kolesnikov, Dirk Weissenborn, Xiaohua Zhai, Thomas Unterthiner, Mostafa Dehghani, Matthias Minderer, Georg Heigold, Sylvain Gelly, Jakob Uszkoreit, and Neil Houlsby. An Image is Worth 16x16 Words: Transformers for Image Recognition at Scale. *International Conference on Learning Representations*, 2021. 2, 4
- [11] Ruo-Nan Duan, Jia-Yi Zhu, and Bao-Liang Lu. Differential entropy feature for EEG-based emotion classification. In *6th International IEEE/EMBS Conference on Neural Engineering (NER)*. IEEE, 2013. 2
- [12] Towfeeq Fairouz and Hedi Khammari. SVM classification of CWT signal features for predicting sudden cardiac death. *Biomedical Physics & Engineering Express*, 2016. 2
- [13] Zhiqiang Fan, Fangyue Chen, Xiaokai Xia, and Yu Liu. EEG Emotion Classification Based on Graph Convolutional Network. *Applied Sciences*, 2024. 2, 3
- [14] Divya Garg and Gyanendra K. Verma. Emotion Recognition in Valence-Arousal Space from Multi-channel EEG data and Wavelet based Deep Learning Framework. *Procedia Computer Science*, 2020. 2, 3
- [15] A. Grossmann and J. Morlet. Decomposition of Hardy Functions into Square Integrable Wavelets of Constant Shape. *SIAM Journal on Mathematical Analysis*, 1984. 4
- [16] Vipin Gupta, Mayur Dahyabhai Chopda, and Ram Bilas Pachori. Cross-subject emotion recognition using flexible analytic wavelet transform from eeg signals. *IEEE Sensors Journal*, 2019. 3
- [17] Xinyun Hu and Gabriel Lodewijks. Exploration of the effects of task-related fatigue on eye-motion features and its value in improving driver fatigue-related technology. *Transportation Research Part F: Traffic Psychology and Behaviour*, 2021. 7
- [18] Md. Rabiul Islam and Mohiuddin Ahmad. Wavelet analysis based classification of emotion from eeg signal. In *International Conference on Electrical, Computer and Communication Engineering*, 2019. 3
- [19] Kinaan Javed, Vamsi Reddy, and Forshing Lui. Neuroanatomy, Cerebral Cortex. In *StatPearls*. StatPearls Publishing, 2024. 7
- [20] Xiao Jiang, Gui-Bin Bian, and Zean Tian. Removal of Artifacts from EEG Signals: A Review. *Sensors*, 2019. 1
- [21] Stamos Katsigiannis and Naeem Ramzan. DREAMER: A Database for Emotion Recognition Through EEG and ECG Signals From Wireless Low-cost Off-the-Shelf Devices. *IEEE Journal of Biomedical and Health Informatics*, 2018. 1
- [22] Diederik P. Kingma and Jimmy Ba. Adam: A Method for Stochastic Optimization. *International Conference on Learning Representations*, 2017. 4
- [23] Sander Koelstra, Christian Muhl, Mohammad Soleymani, Jong-Seok Lee, Ashkan Yazdani, Touradj Ebrahimi, Thierry Pun, Anton Nijholt, and Ioannis Patras. DEAP: A Database for Emotion Analysis ;Using Physiological Signals. *IEEE Transactions on Affective Computing*, 2012. 2, 3
- [24] Bernhard Kratzwald, Suzana Ilić, Mathias Kraus, Stefan Feuerriegel, and Helmut Prendinger. Deep learning for affective computing: Text-based emotion recognition in decision support. *Decision Support Systems*, 2018. 1
- [25] Sunil Kumar and Ilyoung Chong. Correlation Analysis to Identify the Effective Data in Machine Learning: Prediction of Depressive Disorder and Emotion States. *International Journal of Environmental Research and Public Health*, 2018. 1
- [26] Xiang Li, Dawei Song, Peng Zhang, Guangliang Yu, Yuexian Hou, and Bin Hu. Emotion recognition from multi-channel EEG data through Convolutional Recurrent Neural Network. In *2016 IEEE International Conference on Bioinformatics and Biomedicine (BIBM)*, 2016. 3
- [27] Yu Liu, Yufeng Ding, Chang Li, Juan Cheng, Rencheng Song, Feng Wan, and Xun Chen. Multi-channel EEG-based emotion recognition via a multi-level features guided capsule network. *Computers in Biology and Medicine*, 2020. 3
- [28] Nikolai Smetanin Maria Volodina. Cortical and autonomic responses during staged Taoist meditation: Two distinct meditation strategies. *PLOS ONE*, 2021. 4

- [29] Shyam Marjit, Upasana Talukdar, and Shyamanta M Hazarika. EEG-Based Emotion Recognition Using Genetic Algorithm Optimized Multi-Layer Perceptron. In *International Symposium of Asian Control Association on Intelligent Robotics and Industrial Automation*, 2021. 2, 3
- [30] J. Morlet, G. Arens, E. Fourgeau, and D. Glard. Wave propagation and sampling theory—Part I: Complex signal and scattering in multilayered media. *GEOPHYSICS*, 1982. 2, 4
- [31] Robert Oostenveld and Peter Praamstra. The five percent electrode system for high-resolution EEG and ERP measurements. *Clinical Neurophysiology*, 2001. 2
- [32] Varsha Kiran Patil, Vijaya R. Pawar, Shreiya Randive, Rutika Rajesh Bankar, Dhanashree Yende, and Aditya Kiran Patil. From face detection to emotion recognition on the framework of Raspberry pi and galvanic skin response sensor for visual and physiological biosignals. *Journal of Electrical Systems and Information Technology*, 10, 2023. 2
- [33] Jie Quan, Ying Li, Lingyue Wang, Renjie He, Shuo Yang, and Lei Guo. EEG-based cross-subject emotion recognition using multi-source domain transfer learning. *Biomedical Signal Processing and Control*, 2023. 3
- [34] James Russell. A Circumplex Model of Affect. *Journal of Personality and Social Psychology*, 1980. 2
- [35] R. Santhoshkumar and M. Kalaiselvi Geetha. Deep learning approach for emotion recognition from human body movements with feedforward deep convolution neural networks. *Procedia Computer Science*, 2019. PerCAA. 2
- [36] Helen Schneider, Svetlana Pavlitska, Helen Gremmelmaier, and Marius Zöllner. Datasets for valence and arousal inference: A survey. In *IEEE/CVF Conference on Computer Vision and Pattern Recognition (CVPR) Workshops*, 2025. 2
- [37] Jiahui She, Yibo Hu, Hailin Shi, Jun Wang, Qiu Shen, and Tao Mei. Dive into Ambiguity: Latent Distribution Mining and Pairwise Uncertainty Estimation for Facial Expression Recognition. *Conference on Computer Vision and Pattern Recognition*, 2021. 1
- [38] Lin Shu, Yang Yu, Wenzhuo Chen, Haoqiang Hua, Qin Li, Jianxiu Jin, and Xiangmin Xu. Wearable Emotion Recognition Using Heart Rate Data from a Smart Bracelet. *Sensors*, 2020. 2
- [39] M. Soleymani, J. Lichtenauer, T. Pun, and M. Pantic. A Multimodal Database for Affect Recognition and Implicit Tagging. *IEEE Transactions on Affective Computing*, 2012. 2
- [40] Wei Tao, Chang Li, Rencheng Song, Juan Cheng, Yu Liu, Feng Wan, and Xun Chen. EEG-Based Emotion Recognition via Channel-Wise Attention and Self Attention. *IEEE Transactions on Affective Computing*, 2023. 2, 3
- [41] Paweł Tarnowski, Marcin Kołodziej, Andrzej Majkowski, and Remigiusz Jan Rak. Eye-Tracking Analysis for Emotion Recognition. *Computational Intelligence and Neuroscience*, 2020. 7
- [42] Ashish Vaswani, Noam Shazeer, Niki Parmar, Jakob Uszkoreit, Llion Jones, Aidan N. Gomez, Lukasz Kaiser, and Illia Polosukhin. Attention Is All You Need. *31st Conference on Neural Information Processing Systems*, 2023. 4
- [43] Niklas Wagner, Felix Mätzler, Samed Vossberg, Helen Schneider, Svetlana Pavlitska, and J.M. Zöllner. Cage: Circumplex affect guided expression inference. In *IEEE/CVF Conference on Computer Vision and Pattern Recognition (CVPR) Workshops*, 2024. 2
- [44] Zhe Wang, Yongxiong Wang, Chuanfei Hu, Zhong Yin, and Yu Song. Transformers for EEG-Based Emotion Recognition: A Hierarchical Spatial Information Learning Model. *IEEE Sensors Journal*, 2022. 3
- [45] Rui Zhang, Zhenyu Wang, Zhenhua Huang, Li Li, and Mengdan Zheng. Predicting Emotion Reactions for Human-Computer Conversation: A Variational Approach. *IEEE Transactions on Human-Machine Systems*, 2021. 1
- [46] Wei-Long Zheng and Bao-Liang Lu. Investigating critical frequency bands and channels for EEG-based emotion recognition with deep neural networks. *IEEE Transactions on Autonomous Mental Development*, 2015. 2
- [47] Dogancan Şen and Mustafa Sert. Continuous valence prediction using recurrent neural networks with facial expressions and EEG signals. In *Signal Processing and Communications Applications Conference*, 2018. 2, 4